Viscosity of PMMA on Silica: Epitome of Systems with Strong Polymer–Substrate Interactions

ARTICLE *in* MACROMOLECULES · SEPTEMBER 2013

Impact Factor: 5.8 · DOI: 10.1021/ma401527v

4 AUTHORS, INCLUDING:

Fei Chen
Boston University
13 PUBLICATIONS **122** CITATIONS
SEE PROFILE

Chi-Hang Lam
The Hong Kong Polytechnic University
79 PUBLICATIONS **977** CITATIONS
SEE PROFILE

Ophelia KC Tsui
Boston University
107 PUBLICATIONS **2,359** CITATIONS
SEE PROFILE

Macromolecules

Article

pubs.acs.org/Macromolecules

Viscosity of PMMA on Silica: Epitome of Systems with Strong Polymer–Substrate Interactions

Ranxing N. Li,[†,‡] Fei Chen,[†] Chi-Hang Lam,[§,*] and Ophelia K. C. Tsui[†,‡,*]

[†]Department of Physics, Boston University, Boston, Massachusetts 02215, United States

[‡]Division of Materials Science and Engineering, Boston University, Boston, Massachusetts 02215, United States

[§]Department of Applied Physics, Hong Kong Polytechnic University, Hung Hom, Hong Kong

ABSTRACT: We measured the viscosity of poly(methyl methacrylate) (PMMA) films supported by silica, where the carbonyl group on the side chains of the polymer interacts strongly with the hydroxyl groups of the surface. The result shows that the viscosity increases with decreasing film thickness at temperatures above 110 °C, but displays an opposite trend at lower temperatures. A three-layer model, consisting of a mobile top layer, a bulk-like middle layer and an immobile bottom layer was found to fit the data well. A detailed breakdown of the layer contributions to the total mobility unveils that the mobility gain brought about by the top layer is balanced by the mobility loss by the bottom layer at 110 °C. When the temperature is lowered or raised, the balance is offset, in favor, of the top and bottom layer, respectively.

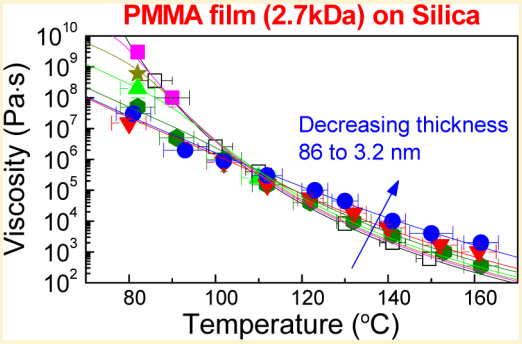

INTRODUCTION

Many existing and emergent technologies make use of polymer nanometer films. Viscosity is an important property that describes how fluidic a material is and, among other things, indicates how easily an item spontaneously deforms upon heating. While the viscosity of bulk polymer melts has been accepted as textbook knowledge for decades, much less is known about the counterpart in nanometer films. In addition to the conformational change anticipated for long-chain polymers upon nanoconfinement, perturbation to the polymer dynamics at an interface is also expected to cause the effective (or average) viscosity of the films to differ from the bulk. Recently we developed a method to determine the effective viscosity of polymer nanometer films by measuring the dynamics of the surface capillary waves in the films.[1,2] The result, obtained from polystyrene (PS) supported by silica, shows that the effective viscosity decreases markedly with decreasing film thickness below ~10 nm. A two-layer model,[1,2] involving hydrodynamic coupling between a thin, mobile layer at the near-air surface exhibiting Arrhenius dynamics and a lower layer exhibiting the same glassy dynamics as the bulk, has been found to explain the data well. This finding echoes those of previous experiments,[3−6] involving a variety of techniques, that the mobility of PS near silica is similar to the bulk,[4] but that near air is noticeably faster.[3−6]

Polystyrene supported by silica is a representative system of polymer films displaying decreasing glass transition temperature, T_g, with decreasing film thickness. In this study, we focus on the viscosity of poly(methyl methacrylate) (PMMA) films supported by silica, a representative of polymer films displaying increasing T_g with decreasing film thickness. Previous studies showed that the near-air mobility of PMMA is also faster than bulk,[7−10] but the near-substrate mobility is slower.[8,9,11] In addition, the substrate can influence the near-air mobility over a distance of up to 250 nm.[10,11] Given these observations, a model consisting of at least three layers is anticipated essential to embrace the full dynamic heterogeneity. In a previous publication,[12] we reported preliminary measurement of these films above the bulk T_g, where the effective viscosity was found to fit well to a two-layer model comprising a bulk-like layer atop a slow substrate layer.[12] In this work, we elaborate and expand the measurements to below the bulk T_g. We find that the effective viscosity demonstrates simultaneous influence of a near-air mobile region and a near-substrate slow region. At temperatures below or close to the bulk T_g the near-air region dominates; otherwise the near-substrate region dominates. A three-layer model, analogous to the two-layer model used before,[1,2,12] is required to describe the result fully.

EXPERIMENTAL SECTION

Poly(methyl methacrylate) with molecular weights, M_w = 2.7K and 12.4K g/mol (polydispersity index (PDI) = 1.09 and 1.08, respectively) are purchased from Polymer Source. The tacticity (%) is i:h:s = 7:24:69, similar to that of atatic PMMA reported by Grohens et al.[13] Silicon (100) wafers covered with a 100 nm thick thermal oxide layer and cut into 1 × 1 cm^2 slides are used for the substrates. Prior to use, the slides are cleaned in a piranha solution (H_2SO_4:H_2O_2 in 7:3 volume ratio) at 140 °C for 20 min followed by thorough rinsing with deionized water and drying with 99.99% nitrogen. Afterward, the substrates are further cleaned in an oxygen plasma for 25 min. PMMA films are spin-coated from solutions of toluene onto the cleaned

Received: July 20, 2013
Revised: September 15, 2013
Published: September 25, 2013

   dx.doi.org/10.1021/ma401527v | *Macromolecules* 2013, 46, 7889−7893

substrates. The film thickness is determined by using a single-wavelength (633 nm) Stokes ellipsometer by Gaertner Scientific Corp. (Skokie, IL) at multiple locations on the films. The deviations in the thickness measurements are usually less than 0.3 nm. The same ellipsometer is also used to determine the T_g of a film. Before a T_g measurement, the specimen is preannealed at 130 °C for 4 h. Then the ellipsometric angles Δ and Ψ are recorded as the temperature, T, is swept between 130 and 20 °C three times (down, up, down) at 2 °C/min. In each temperature sweep, T_g is determined to be the midpoint where $d\Delta/dT$ or $d\Psi/dT$ shows a step change.[14] The specimen T_g and the associated uncertainty is estimated from the average and standard deviation, respectively.

Figure 1 shows the thickness (h) dependence of the T_g of the PMMA2.7K films. As seen, for h > 100 nm the T_g approaches a

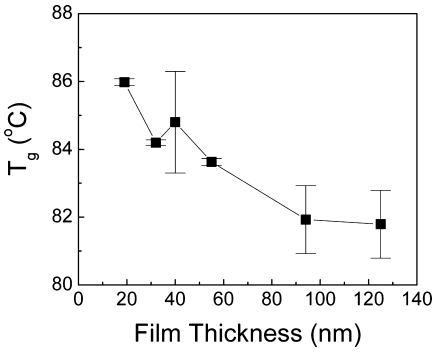

Figure 1. Glass transition temperature, T_g, versus film thickness, h, of the PMMA2.7K films.

constant of ~82 °C. But when h is decreased below 100 nm, the T_g increases with decreasing h. At h = 20 nm, the ratio, $T_g(h)/T_g(\infty)$ (where the T_g's are expressed in kelvin) reaches 1.01. This dependence agrees with that reported for the same system with a higher M_w of 100 K g/mol.[15] Independence of $T_g(h)$ on M_w is in keeping with hitherto findings.[15−17]

Following our previous approach,[1,18−20] we measure the effective viscosity of the as-cast films by studying the dynamics of the surface capillary waves and model the data by assuming the films to be viscous. (c.f. The entanglement M_w of PMMA as estimated from the onset of reptation dynamics is ~30K g/mol and bigger than the M_w's used here[21]). To avoid thermal degradation, we keep the films under nitrogen for measurements taken above 140 °C. As noted before,[1,18−20] the films roughen upon heating. We characterize the roughening process by studying the temporal evolution of the power spectral density (PSD), which we obtain by radial averaging the Fourier transformation of the surface topography of the film (obtained by atomic force microscopy) upon multiplying it by a Welch function. Further details of the procedure can be found in refs 1 and 18. It has been shown that the PSD varies initially with time, t, according to[1,18−20]

$$A_q^2(t) = A_q^2(0) + \left[\frac{k_B T}{d^2G/dh^2 + \gamma q^2} - A_q^2(0)\right](1 - \exp(2\Gamma_q t)) \quad (1)$$

where $A^2_q(t)$ denotes the PSD, q is the wavevector, k_B is the Boltzmann constant; γ and $G(h)$ is the surface tension and van der Waals potential of the film;[22] Γ_q is the relaxation rate of the surface capillary mode with wavevector q and given by

$$\Gamma_q = -Mq^2(\gamma q^2 + d^2G/dh^2) \quad (2)$$

where M is the total mobility of the film, defined to be the planar fluid current density generated in the film integrated over the film thickness per unit planar pressure gradient applied.[1,20] Accordingly, the dynamics of the surface capillary waves (eq 2) manifests the dynamics of the whole film, not just the surface region. If the film possesses no dynamic heterogeneity, its viscosity η is related to M by $M = h^3/(3\eta)$.[20] But if there is heterogeneity, the value of η deduced from this relation, as in here, represents an average value that is referred to as the effective viscosity. To model the PSD data, we first make use of the fact that $\lim_{q\to\infty} A^2_q(t) = k_BT/(\gamma q^2)$.[23] Therefore, γ can be determined by fitting the high q portion of the PSDs to this expression. The fitted values obtained typically lie between 0.03 and 0.05 N/m, so are consistent with published values.[24] To determine the value of η, we fit the full PSD curves to eq 1 (with M replaced by $h^3/(3\eta)$) using η as the only fitting parameter while keeping γ to the fitted value obtained as described above; h and T to the experimental values; and d^2G/dh^2 to 1.3 times the value calculated by using the theory of Dzyaloshinskii, Lifshitz, and Pitaevskii.[22] This choice of d^2G/dh^2 is found to optimize the fits attempted for the data of the 3 nm films between 130 ≤ T ≤ 150 °C when η and d^2G/dh^2 are covaried. For the thicker films, the fitted value of η is much less sensitive to the choice of d^2G/dh^2. Figure 2 shows a representative sequence of PSD's (symbols) we obtain. As seen, it agrees reasonably well with eq 1 (solid lines).

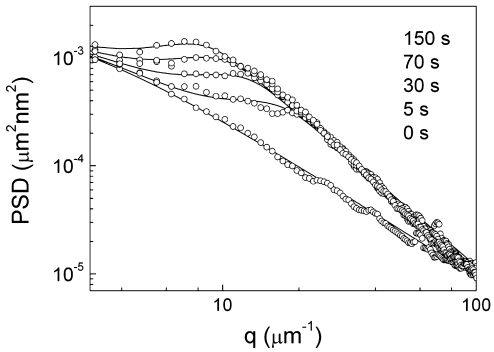

Figure 2. Timed-sequence of power spectral density (PSD) taken from an 8 nm PMMA2.7K film at 130 °C (symbols). The annealing times of the PSD curves are (from bottom to top): 0, 5, 30, 70, and 150 s. The solid lines represent the best fit to eq 1 obtained as described in the text.

RESULTS AND DISCUSSION

We first examine the effective viscosity η of the PMMA2.7K films. The result, displayed in Figure 3a, shows that the data of the 86 nm films are consistent with the bulk viscosity. As the film thickness is decreased, the temperature dependence of η becomes weaker, consistent with previous findings of nano-confined systems.[1,25−27] In addition, for T > 110 °C η increases with decreasing film thickness, consistent with the thickness dependence of T_g. But for T < 110 °C, it displays an opposite trend except for the data of the h = 3.2 nm films. The opposite thickness variations observed in different temperature regions suggest that the films simultaneously possess a slow and a mobile component, with one component dominating the effective viscosity in one region. By using fluorescent labeling, Priestley et al. studied the local aging rate at different depths of the PMMA films.[8] The result implies that there is enhanced cooperative segmental mobility near the air surface, but almost complete suppression of aging near the substrate surface, which is likely caused by impediments by the interfacial hydrogen bonds. We propose a similar three-layer model to explain our result.

In our model, we assume the films to comprise three layers: a mobile top layer, a glassy bulk-like middle layer and a bottom dead (i.e., immobile) layer. We denote quantities associated with the top, glassy and dead layers by subscripts t, g, and d, respectively. Assuming uniform viscosity in each layer and the

dx.doi.org/10.1021/ma401527v | Macromolecules 2013, 46, 7889−7893

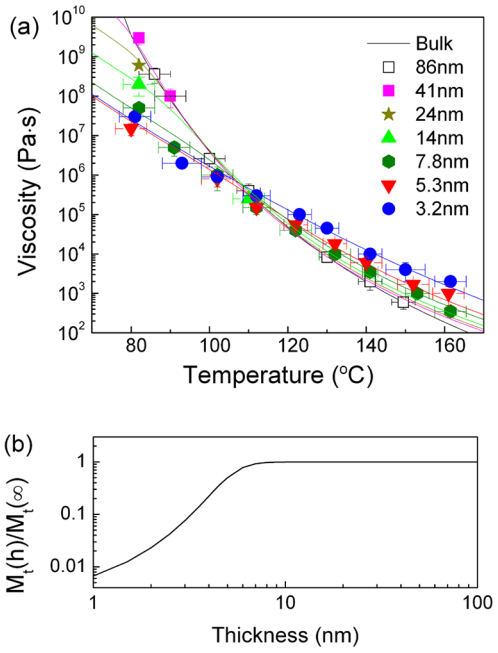

Figure 3. (a) Viscosity vs temperature for PMMA2.7K films with different thicknesses as indicated in the legend. The solid lines are the best fit to the three-layer model as described in the text. (b) Functional form of the thickness dependent surface mobility, $M_t(h)$, used in the three-layer model fit shown in part a.

no-slip boundary condition at each interface, the film mobility is given by[1]

$$M = \frac{h_g^3}{3\eta_g} + \frac{h_t^3}{3\eta_t} + \frac{h_t h_g (h_g + h_t)}{\eta_g} \quad (3)$$

where h_i and η_i denotes the thickness and viscosity, respectively, of layer i and $h \equiv h_t + h_g + h_d$. Equation 1 can be rewritten as the sum of two terms[12]

$$M = \frac{(h - h_d)^3}{3\eta_g} + M_t \quad (4)$$

where $M_t \equiv h_t^3(\eta_g^{-1} - \eta_t^{-1})/3$, and is expected to be $\approx h_t^3/(3\eta_t)$, i.e., the mobility of the surface layer. (As we shall see shortly, $M_t(T)$ is Arrhenius, quite unlike $\eta_g(T)$.) The other term is the mobility of the film had it been uniform with viscosity η_g minus the mobility loss due to trimming by the dead layer. We find that eq 4 provides a good description to the data (Figure 3a) if we assume the published viscosity of bulk PMMA2.7K for η_g,[21] $h_d = 2.2 \pm 1$ nm and an Arrhenius form times a thickness-dependent multiplicative factor $r(h)$ for M_t, where

$$r(h) = \frac{M_t(h)}{M_t(\infty)} = \frac{1}{1 + \exp[-(h - l_t)/\Delta l_t]} \quad (5)$$

This form of $r(h)$ implies that when the film thickness h is $\ll l_t$, the surface mobility M_t decays with decreasing h at a decay length of Δl_t. In other words, when the upper surface is brought toward the bottom surface by a distance of l_t or less, the surface mobility begins to decay at a decay length of Δl_t. The fitted expression of $M_t(\infty)$, and values of l_t and Δl_t are given in Table 1. Figure 3b displays the functional form of $r(h)$. As h is decreased from the far right, $r(h)$ starts to decrease from 1

Table 1. Summary of the T_g and Three-Layer Model Fitting Results of the PMMA Films

	PMMA2.7K	PMMA12.4K
$T_g(h\to\infty)$ (°C)	82 ± 3	100 ± 3
$M_t(h=\infty)$ (m^3 Pa^{-1} s^{-1})	3.5×10^{-11} exp(−149 kJ/mol/RT)	0.011 exp(−240 kJ/mol/RT)
l_t (nm)	5 ± 1	4.6 ± 1
Δl_t (nm)	0.8 ± 1	1 ± 1
h_d (nm)	2.2 ± 1	1.8 ± 1

when h approaches 7 nm and declines rapidly to 0.02 near $h = 2$ nm before coming to a steady value. Given the form of $r(h)$, the mobility of the 3.2 nm film is suppressed strongly, that of the 5 nm films mildly, and that of the $h > 10$ nm films negligibly. This accounts for the peculiar trend reversal seen in the thickness dependence of η around $h = 5.3$ nm at low temperatures (Figure 3a). Most probably, the suppression of M_t arises from the influence of the substrate on the chain dynamics at the air surface, which was also found in surface nanohole relaxation[10] and surface T_g[11] measurements. We note that while the maximum range of the substrate effect as found in these studies was up to 250 nm, the range at which the surface mobility declined the fastest actually occurred within 25 nm. This is about 5 times the range found here. We surmise that the extent of surface sensitivity depends on the dynamics being probed, similar to the different thicknesses found of the surface mobile layer by different methods.[4,5,28]

As discussed above, a two-layer model is able to model the effective viscosity of PS supported by silica.[1,2] Compared to the present three-layer model (eq 4), the two-layer model differs in two respects. First, it does not possess a dead layer, i.e., $h_d = 0$. Second, the surface mobility M_t does not depend on h, i.e., $r(h) \equiv M_t(h)/M_t(\infty) = 1$ down to 3.2 nm. We examine how these differences are manifest in the data. Shown in Figure 4 are plots of $M(h)/M(3.2\text{ nm})$ versus h, where $M(3.2\text{ nm})$ is the best fitted Arrhenius line to the 3.2 nm data. In part (a), we display the data acquired at low temperatures ($T < 100$ °C) where M_t dominates. In part (b), we display the data at higher temperatures where the mobility of the glassy layer is non-negligible and the effect of the dead layer is important.

In these graphs, we also show the best fit to the full three-layer model (solid lines), the same model except for $r(h)$ being set equal to 1 (dotted lines with open triangles), and h_d and M_t set equal to zero (dashed lines). In comparing the solid and dotted lines with open triangles, one sees that $r(h)$ affects M solely in the lowest-h region. Comparing the dashed and dotted lines, one sees that the effect of the dead layer or h_d is negligible at low temperatures as expected since M_t dominates there. At high temperatures where the first term of eq 4 is no longer small compared to M_t, the dead layer causes M to exhibit a super h^3 dependence (Figure 4b). Because the effective viscosity η is given by $\eta = h^3/(3M)$, a super h^3 dependence in M renders η a decreasing function of h and explains the high-temperature behavior seen in Figure 3a. Similarly, at low temperatures where M is sub h^3 for $5 < h < 50$ nm and ~h^3 otherwise (Figure 4a), the data in Figure 3a reverses trend. At $T = 110$ °C, the dashed and solid lines in Figure 4b approach each other at small h, signifying cancellation of the opposites effects of the surface and substrate layers. In tandem, the $\eta-T$ curves in Figure 3a converge near this temperature.

To explore if the length scales of our model, i.e., h_d, l_t or Δl_t change with the molecular weight of the films, we measure the

dx.doi.org/10.1021/ma401527v | Macromolecules 2013, 46, 7889−7893

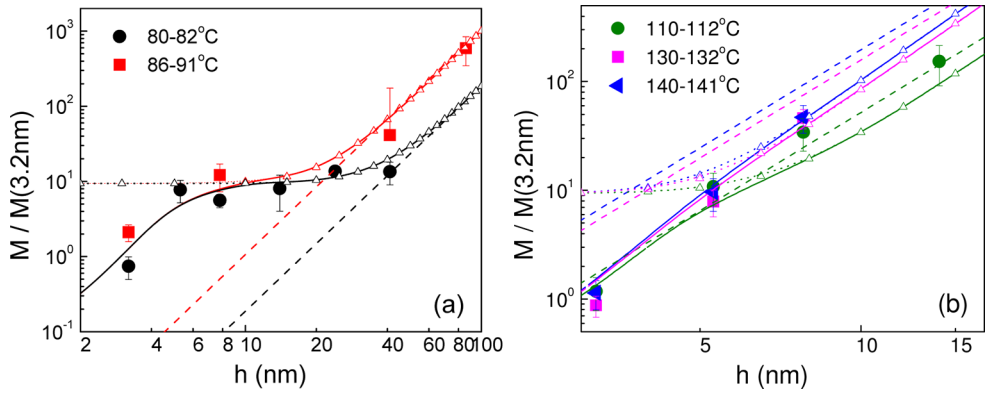

Figure 4. (a) Normalized total mobility, $M(h)/M(3.2\text{ nm})$ versus film thickness, h, in the low ($T < 100$ °C) (a) and high temperature ($T > 100$ °C) region (b). The solid lines denote the three-layer model fit (eq 4). The dotted lines with open triangles denote the model lines with $r(h)$ set equal to 1. The dashed lines denote the model lines with both h_d and M_t set equal to 0.

viscosity of PMMA films with a ∼4-fold higher M_w of 12.4K g/mol. We find that while the effective viscosity of these films is higher, the thickness variation is essentially unchanged given the uncertainties of h_d, l_t, and Δl_t (Table 1). This is in keeping with previous findings that the range of dynamic heterogeneity at an interface does not change noticeably with the M_w of the films.[2,5,10]

In this analysis, we have assumed the near-air and near-substrate layers to be uniform, exhibiting abrupt transition to the middle layer. In reality, these layers are probably inhomogeneous. Given the thickness dependence of M_t found above, the transition of the near-air layer to those below should be gradual, extending over a distance of ∼10 nm. Such a picture is more in line with a gradient layer structure as implied in the result of depth-dependent T_g measurement[4] and computer simulation.[29] But it would require our reinterpreting h_d, l_t, and Δl_t to be average values, affording only a crude picture of the layer structure. In addition, any modifications in the dynamics of the middle region by the substrate may also be manifest in the thickness-dependence found here of the surface mobility since the surface mobile layer in the three-layer model description may embrace part of or all of the middle layer if the boundary between them is actually blurred. Despite these possible limitations, the overarching effect of the interfaces as informed by our analysis should be general, as any viable model must give the same total mobility $\eta(h, T)$ found in experiment.

CONCLUSION

In conclusion, we have measured the effective viscosity of PMMA films supported by silica. We find that the data can be accounted for by a three-layer model comprising a mobile top layer, bulklike middle layer and an immobile substrate layer. In addition, the mobility of the top layer demonstrates a reduction with decreasing film thickness, which we attribute to the influence of the substrate surface. The balance between the layer contributions to the total mobility of the films has been as such that the substrate layer dominates at temperatures above 110 °C, but the surface layer supersedes at lower temperatures. This leads to an intriguing reversal in the thickness dependence of the thin film viscosity in different temperature regions.

AUTHOR INFORMATION

Corresponding Authors

*E-mail: (O.K.C.T.) okctsui@bu.edu.
*E-mail: (C.H.L.) C.H.Lam@polyu.edu.hk.

Notes

The authors declare no competing financial interest.

ACKNOWLEDGMENTS

O.K.C.T. is grateful to the support of National Science Foundation through Projects DMR-1004648 and DMR-1310536. C.H.L. expresses thanks for the support of HK PolyU via Project G-YJ71.

REFERENCES

(1) Yang, Z.; Fujii, Y.; Lee, F. K.; Lam, C.-H.; Tsui, O. K. C. *Science* **2010**, *328*, 1676−1679.
(2) Yang, Z.; Clough, A.; Lam, C.-H.; Tsui, O. K. C. *Macromolecules* **2011**, *44*, 8294−8300.
(3) Tanaka, K.; Takahara, A.; Kajiyama, T. *Macromolecules* **1997**, *30*, 6626−6632.
(4) Ellison, C. J.; Torkelson, M. *Nat. Mater.* **2003**, *2*, 695−670.
(5) Paeng, K.; Swallen, S. F.; Ediger, M. D. *J. Am. Chem. Soc.* **2011**, *133*, 8444−8447.
(6) Fakhraai, Z.; Forrest, J. A. *Science* **2008**, *319*, 600−604.
(7) Roth, C. B.; Dutcher, J. R. *Eur. Phys. J. E* **2003**, *12*, 103−107.
(8) Priestley, R. D.; Ellison, C. J.; Broadbelt, L. J.; Torkelson, J. M. *Science* **2005**, *309*, 456−459.
(9) Priestley, R. D.; Mundra, M. K.; Barnett, N. J.; Broadbelt, L. J.; Torkelson, J. M. *Aust. J. Chem.* **2007**, *60*, 765−771.
(10) Qi, D.; Fakhraai, Z.; Forrest, J. A. *Phys. Rev. Lett.* **2008**, *101*, 096101.
(11) Roth, C. B.; McNerny, K. L.; Jager, W. F.; Torkelson, J. M. *Macromolecules* **2007**, *40*, 2568−2574.
(12) Peng, D.; Li, R. N.; Lam, C.-H.; Tsui, O. K. C. *Chin. J. Polym. Sci.* **2013**, *31*, 12−20.
(13) Grohens, Y.; Brogly, M.; Labbe, C.; Marie-Odile, D.; Schultz, J. *Langmuir* **1998**, *14*, 2929−2932.
(14) Clough, A.; Peng, D.; Yang, Z.; Tsui, O. K. C. *Macromolecules* **2011**, *44*, 1649−1653.
(15) Keddie, J. L.; Jones, R. A. L.; Cory, R. A. *Faraday Discuss.* **1994**, *98*, 219−230.
(16) Tsui, O. K. C.; Zhang, H. F. *Macromolecules* **2001**, *34*, 9139−9142.
(17) Ellison, C. J.; Mundra, M. K.; Torkelson, J. M. *Macromolecules* **2005**, *38*, 1767−1778.
(18) Tsui, O. K. C.; Wang, Y. J.; Lee, F. K.; Lam, C.-H.; Yang, Z. *Macromolecules* **2008**, *41*, 1465−1468.
(19) Peng, D.; Yang, Z.; Tsui, O. K. C. *Macromolecules* **2011**, *44*, 7460−7464.
(20) Lam, C.-H.; Tsui, O. K. C.; Peng, D. *Langmuir* **2012**, *28*, 10217−10222.
(21) Berry, G. C.; Fox, T. G. *Adv. Polym. Sci.* **1968**, *5*, 261−357.

(22) Zhao, H.; Wang, Y. J.; Tsui, O. K. C. *Langmuir* **2005**, *21*, 5817−5824.
(23) Yang, Z. H.; Wang, Y.; Todorova, L.; Tsui, O. K. C. *Macromolecules* **2008**, *41*, 8785−8788.
(24) Jones, R. A. L.; Richards, R. W. R., *Polymers at Surfaces and Interfaces*; Cambridge University Press: Cambridge, U.K., 1999.
(25) Fakhraai, Z.; Forrest, J. A. *Phys. Rev. Lett.* **2005**, *95*, 025701.
(26) Schonhals, A.; Goering, H.; Schick, C.; Frick, B.; Zorn, R. *J. Non-Cryst. Solids* **2005**, *351*, 2668−2677.
(27) Koh, Y. P.; Simon, S. L. *J. Polym. Sci., Part B: Polym. Phys.* **2008**, *46*, 2741−2753.
(28) Ilton, M.; Qi, D.; Forrest, J. A. *Macromolecules* **2009**, *42*, 6851−6854.
(29) Peter, S.; Meyer, H.; Baschnagel, J.; Seemann, R. *J. Phys.: Condens. Matter* **2007**, *19*, 205119.